No changes in myocardial perfusion following radiation therapy of left-sided breast cancer: A positron emission tomography study

Thomas Rasmussen, MD, PhD,[a] Andreas Kjær, MD, PhD, DMSc,[a] Martin Lyngby Lassen, MSc, PhD,[a] Anders Navrsted Pedersen, MD, PhD,[b] Lena Specht, MD, DMSc,[b] Marianne C. Aznar, MSc, PhD,[b] and Philip Hasbak, MD, DMSc[a]

[a] Department of Clinical Physiology, Nuclear Medicine & PET and Cluster for Molecular Imaging, Rigshospitalet and University of Copenhagen, Copenhagen, Denmark
[b] Department of Oncology, Rigshospitalet University of Copenhagen, Copenhagen, Denmark

Received Jan 15, 2019; accepted Oct 22, 2019
doi:10.1007/s12350-019-01949-9

Background. **Adjuvant radiation therapy (RT) for breast cancer has improved overall survival. However, incidental exposure of the heart has been linked to development of radiation-induced heart disease. The aim of this study was, in a cohort of asymptomatic post-irradiation breast cancer patients, to investigate changes in myocardial blood flow (MBF) and presence of perfusion defects in myocardial perfusion positron-emission-tomography (PET) in the irradiated myocardium.**

Methods and Results. **Twenty patients treated with RT for left-sided breast cancer underwent ^{13}N-ammonia myocardial perfusion PET 7(± 2) years after breath adapted RT to a total dose of 48 Gy given in 24 fractions. No differences in rest or stress MBF were noted between the irradiated and non-irradiated myocardium (1.29 (± 0.29) vs 1.33 (± 0.29) mL/g/min, ns; 2.74 (± 0.59) vs 2.78 (± 0.66) mL/g/min, ns, respectively). One patient demonstrated a myocardial perfusion defect localized in the irradiated anterior wall myocardium.**

Conclusion. **Although limited by a small sample size, early signs of cardiac injury detected by NH_3 myocardial perfusion PET was at least not frequent in our cohort of patients treated with a modern RT technique for left-sided breast cancer, even 7 years after treatment. The findings however, may not rule out subsequent development of myocardial injury. (J Nucl Cardiol 2021;28:1923–32.)**

Key Words: Myocardial perfusion • ammonia cardiac PET • cardiac positron-emission-tomography • breast cancer • radiation therapy

Abbreviations

CACS	Coronary Artery Calcium Score
CT	Computed tomography
CVD	Cardiovascular disease
LAD	Left anterior descending artery
MBF	Myocardial blood flow
MFR	Myocardial flow reserve
NH_3	Ammonia
PET	Positron-emission-tomography
RCA	Right coronary artery
RT	Radiation therapy

Electronic supplementary material The online version of this article (https://doi.org/10.1007/s12350-019-01949-9) contains supplementary material, which is available to authorized users.

The authors of this article have provided a PowerPoint file, available for download at SpringerLink, which summarizes the contents of the paper and is free for re-use at meetings and presentations. Search for the article DOI on SpringerLink.com.

The authors have also provided an audio summary of the article, which is available to download as ESM, or to listen to via the JNC/ASNC Podcast.

Reprint requests: Thomas Rasmussen, MD, PhD, Department of Clinical Physiology, Nuclear Medicine & PET and Cluster for Molecular Imaging, Rigshospitalet and University of Copenhagen, Copenhagen, Denmark; *drrasmussen@hotmail.com*

1071-3581/$34.00

Copyright © 2019 American Society of Nuclear Cardiology.

See related editorial, pp. 1933–1935

INTRODUCTION

Breast cancer is one of the most frequent types of cancer in women worldwide.[1] Treatment often consists of a combination of surgery, systemic therapy and post-operative adjuvant radiation therapy (RT), either to the breast/chest wall alone or with the addition of regional lymph nodes. Increasing the treatment volume to include regional nodes has been shown to increase survival in some patients but also increases the dose received by the heart and lung.[2–7]

It has long been known that both anthracycline-based chemotherapy and high radiation doses to the heart can cause cardiac injury.[8] However, recent studies indicate that also even relatively small radiation exposures can cause damage.[9] Accordingly, numerous meta-analyses have shown that women suffering from breast cancer, left-sided in particular, exposed to RT are at an increased risk of developing cardiovascular disease (CVD).[2,10–12] The increase in CVD risk seems directly proportional to the mean heart radiation dose and the volume of the heart included in the RT field.[13] High radiation exposures may cause cardiac alterations as early as months after RT, whereas small radiation exposures may not manifest until decades after completed RT.[13,14]

Substantial efforts have been invested in reducing the radiation exposure to the heart to minimize the risk of adverse myocardial events following RT in patients with breast cancer. Modern RT is carried out by three-dimensional computed tomography (CT) planning using conformal treatment techniques. Treatment planning software now includes highly accurate algorithms for calculation of the absorption and scattering of the radiation in the tissues. The algorithm enables calculation of the delivered radiation dose in every point in the patient, taking into account tissue inhomogeneity using the measured Hounsfield units. This approach has led to a reduction in the radiation dose to the heart and, potentially, reduced risk of cardiotoxicity.[15,16] Newer techniques employs breath adapted RT where the breast region is only irradiated in deep inspiration, thus reducing the radiation to the myocardium by moving the heart away from the irradiated chest wall. This technique has been shown to reduce the radiation dose to the heart even further, without compromising the dose to the target.[17–21]

While the clinical manifestations of RT-induced cardiac injuries often do not appear until many years later, application of surrogate markers of cardiac disease can prove useful to not only detect and treat asymptomatic cardiac disease in the individual patient but also to permit an evaluation and guide for current and future RT techniques.[10,14,22,23]

Myocardial perfusion imaging employing positron-emission-tomography (PET) facilitates non-invasive detection of manifested myocardial ischemia as well as coronary microvascular disease, an early indication of endothelial dysfunction. Both of these alterations in the regional myocardial perfusion are predictors of long-term cardiac risk and proof of an on-going process in the epicardial arteries or the myocardial microvasculature.[24]

Due to the long latency of radiation-induced heart disease, the majority of meta-analyses have been conducted on data from patients treated with outdated radiation techniques. More recent studies have suggested that the risk associated with modern RT techniques is considerably lower, especially in women with no other cardiac risk factor.[25] Hence, an evaluation of modern radiation techniques is warranted. Therefore, our aim was to (1) compare myocardial blood flow (MBF) in the irradiated part of the anterior wall myocardium with the non-irradiated inferior wall, and to (2) evaluate the frequency of myocardial defects in myocardial perfusion PET in asymptomatic patients treated with modern radiation techniques for left-sided breast cancer.

MATERIALS AND METHODS

Twenty breast cancer patients in remission after primary treatment were enrolled in this study. The study was approved by the Scientific Ethical Committee of the Capital Region in Denmark (project H-3-2010-066). The inclusion criteria were: adjuvant loco-regional RT for left-sided breast cancer after radical breast conserving surgery (13 patients) or RT after mastectomy (7 patients) and axillary lymph node dissection, treatment completed > 4 years ago, age >49 years, $> 1\%$ of the heart volume received > 10 Gy according to the approved radiation treatment dose plan. The exclusion criteria were: preexisting cardiac disease or thoracic radiotherapy prior to the planned RT for breast cancer, or non-compliance with the investigational procedure (i.e. claustrophobia). After written informed consent patients entered the study consecutively in 2011-2012.

Screening for Cardiovascular Risk Factors

Each patient was screened for cardiac risk factors on the basis of a predefined test panel including body mass index (BMI), smoking habits, alcohol habits, preexisting cardiac disease, hypercholesterolaemia, hypertension, diabetes, cardiac family history, medication, and any early/intermediate radiation side effects.

Computed Tomography and Coronary Artery Calcium Scores

Calcium scoring computed tomography was performed as an electro-cardiogram-gated scan using the vendor's standard protocol with a hybrid PET-CT scanner Siemens Biograph-16 TruePoint PET/CT (Siemens Healthcare, Knoxville, USA).

Scans were performed supine after full inspiration with caudocranial scan direction including the entire heart and upper abdomen with a low-dose technique. Data were reconstructed with a section width of 3 mm and coronary artery calcium scores (CACS) were assessed using a CACS module for Syngo.Via (Siemens, Knoxville, USA) and reported as Agatston scores. Furthermore, CACS was divided into three groups according to CACS (CACS = 0, CACS = 1-400 and CACS > 400) as suggested by American College of Cardiology Foundation/American Heart Association or ACCF/AHA.[26] In two cases images for CACS analysis could not be retrieved.

NH_3 Myocardial Perfusion Positron-Emission-Tomography

Each patient underwent a two-phase, rest and adenosine stress, PET scan with the use of Nitrogen-13 ammonia (^{13}N-NH_3) as the perfusion radiotracer (Figure 1). All image data were acquired in list mode on a Siemens Biograph-16 TruePoint PET/CT (Siemens Healthcare, Knoxville, USA) with the TrueV option (axial field of view of 21.6 cm). Patients were instructed to fast overnight and to avoid the consumption of methylxantine-, caffeine-containing beverages and medications for at least 16 hours before the study. Prior to the rest perfusion scans, a CT-based transmission scan (130 kVp; 25 ref.mAs; helical scan mode with a pitch of 0.95) was obtained during normal breathing for correction of PET photon attenuation. Co-registration of the CT attenuation map with the PET images was verified visually and alignment was corrected when necessary by an experienced nuclear medicine technician. During rest, myocardial perfusion was assessed using 370 MBq of ^{13}N-NH_3. Imaging lasted for 10 minutes and began simultaneously with peripheral injection of the radiotracer. The ^{13}N-NH_3 was administered as a single intravenous bolus (8-10 seconds with infusion rate 0.4 mL/s) followed by a 10 mL saline flush. Pharmacologic stress imaging was performed 50 minutes later and started with a 6-minutes adenosine infusion through a peripheral vein (140 mg/kg/min). A second dose of ^{13}N-NH_3 (370 MBq) was injected three minutes into the administration of adenosine and image acquisition was started simultaneously. Static, dynamic, and 8-bin ECG-gated images were generated from the list mode data. Patient emission data was reconstructed using 3D attenuation weighted ordered subsets expectation maximization (OSEM3D) reconstruction with 168 × 168 matrix, zoom 2, Gaussian filter with a full width at half maximum of 5 mm, 2 iterations, and 21 subsets for gated, static and dynamic images. CT-based attenuation, scatter, decay, and random corrections were applied to the reconstructed images. Dynamic images were reconstructed with 21 frames for rest and stress: 12 × 10, 6 × 30, 2 × 60, 1 × 180 seconds.

Quantitative Perfusion Based on the dynamic subsets, left ventricular contours were assigned automatically using the SyngoMBF software (Siemens Medical Solutions, Berlin, Germany) with minimum observer intervention when appropriate. With a previously described 2-compartment kinetic model for ^{13}N-NH_3, stress and rest flow values in mL/g/min were computed for each sample on the polar map through the resulting time-activity curves for global quantification.[27] Myocardial flow reserve (MFR) was calculated as the ratio between the MBF during stress (sMBF) and MBF during rest (rMBF). rMBF was corrected for the rate pressure product (RPP). The left ventricle was divided into 17 segments according to the AHA 17-segment model and MFR and MBF were calculated.[28]

Four representative segments of the 17-segment model were chosen to define either anterior or inferior wall myocardium to assess differences between the two (Figure 2).[28] Accordingly, segments 7, 8, 13 and 14 and segments 10, 11, 15 and 16 were chosen to define anterior (irradiated) and inferior wall (non-irradiated) myocardium, respectively.

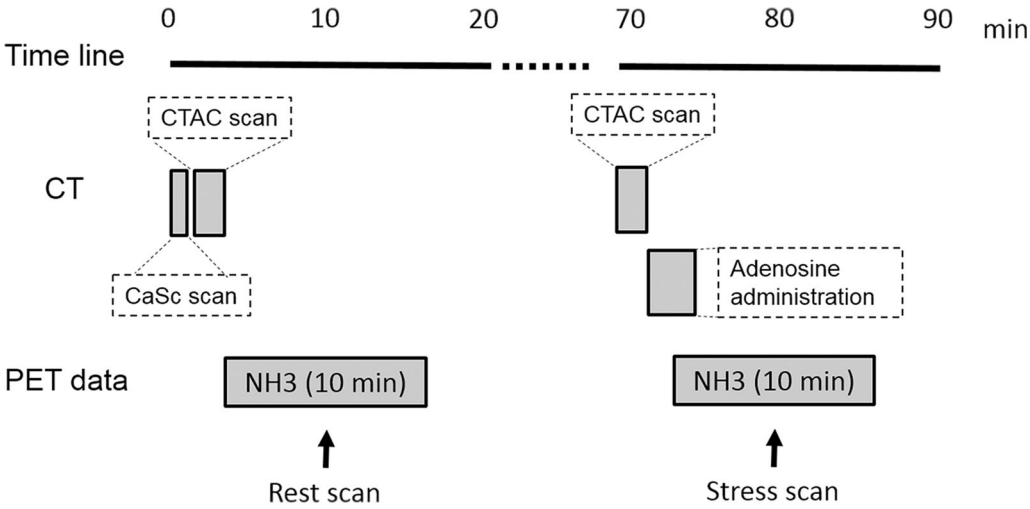

Figure 1. Diagram of scan protocol.

Radiotherapy

All patients had been scanned and treated in the supine position. Respiratory gating was applied as an audio-coached enhanced free breathing end-inspiration technique (as described by Damkjær et al).[29] The clinical target volumes comprised the residual breast/chest wall, the ipsilateral internal mammary lymph node chain from intercostal space 1 through 4, the axillary nodes in level 2-3, and the supraclavicular nodes. The heart had generally not been contoured for the delivered plans following the standard procedure at Rigshospitalet at the time, which limited the dose to the left anterior descending coronary artery (LAD) as a surrogate. The treatment technique comprised a 3-dimensional conformal technique with an anterior supraclavicular photon field and either two thoracic tangential photon fields with an abutting medial electron field or wide tangential photon fields only. The prescription dose was 48 Gy in 24 fractions with 5 fractions/week. Furthermore, the majority of patients received adjuvant antihormonal therapy during and after radiotherapy.

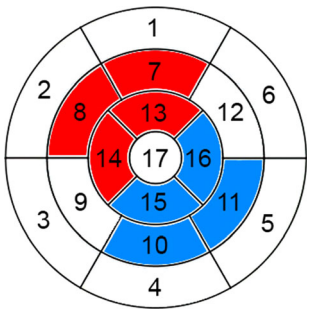

Figure 2. Representative segments of the 17-segment model defining anterior (red) and inferior (blue) wall Myocardium.

PATIENT SELECTION

To ensure that the included patients met the inclusion criteria of > 1% of the heart receiving > 10 Gy, each treatment plan was retrospectively analyzed. By visual inspection it was clear that the heart volume receiving > 10 Gy by far exceeded 1% in all cases. A representative case is shown in Figure 3; from the treatment plan (shown in color wash) it is evident that the high dose levels (shown in red) were deposited in the anterior part of the left ventricle, as expected. The dose volume histogram (DVH) (upper right panel) demonstrates that approximately 13% of the heart (yellow line) received > 10 Gy. Comparison dose volume histograms for the LAD and the RCA are also shown in pink and cyan, respectively, in the DVH (Figure 3, top right).

Figure 4 demonstrates an overlay of the volume receiving > 30 Gy with the corresponding slice of the PET scan. In this case, a considerable part of the left ventricle is included in the volume receiving at least 30 Gy.

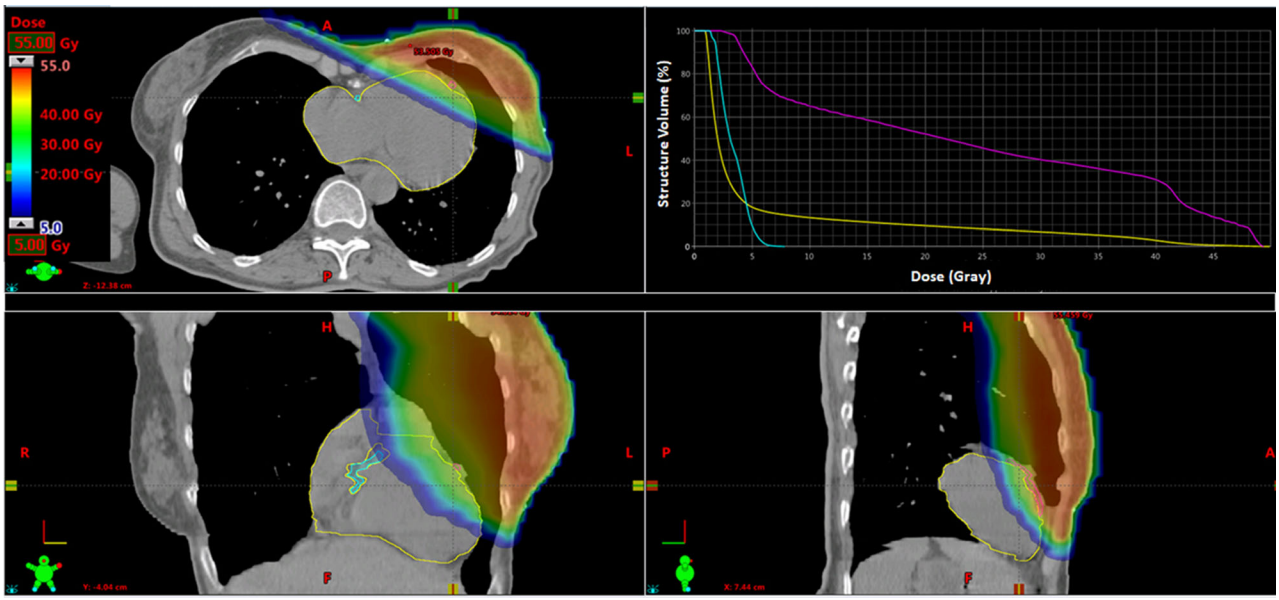

Figure 3. Treatment plan for patient treated for left-sided breast cancer, treated with breast conserving surgery. Axial (upper left), coronal (lower left), and sagittal (lower right) CT-slices. Doses shown from low (blue) to high (= prescribed dose) (red). Dose-volume histogram (upper right) shows radiation doses to the heart (yellow), the left anterior descending coronary artery (LAD) (pink) and the right coronary artery (RCA) (cyan).

STATISTICAL ANALYSIS

Categorical variables were expressed as percentages and continuous variables were reported as means and standard deviations. Differences in characteristics between groups were assessed with the χ^2 test for discrete variables and students *t*-test for continuous variables. Differences in MBF and MFR between the anterior and inferior wall myocardium in the individual patient were assessed with paired *t*-tests. A two tailed *P*-value <0.05 was considered statistically significant. Statistical analyses were performed using SAS® for Windows, version 9.4 (SAS institute, Cary, North Carolina).

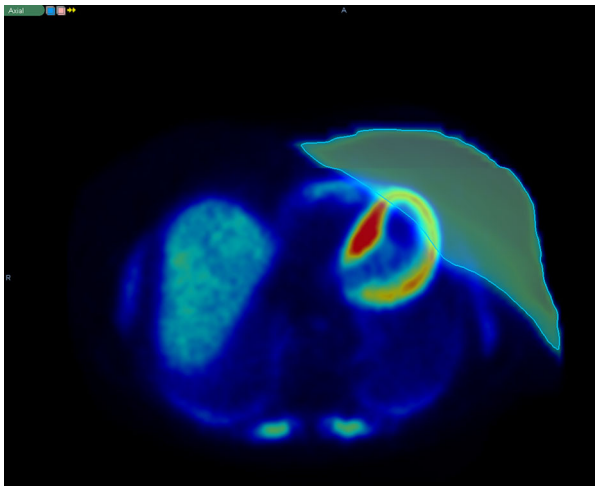

Figure 4. Overlay of the > 30 Gy radiation dose level with the PET scan.

RESULTS

Baseline Characteristics

Baseline characteristics including risk factors for ischemic heart disease are given in Table 1.

CACS and ^{13}N-NH_3 Myocardial Perfusion PET

Categorial CACS values are given in Table 2. Median CACS was 4 and calcifications were primarily located to LAD ($P < 0.001$, data not shown).

MBF and MFR in the anterior vs inferior wall myocardium are given in table 3. Mean global myocardial blood flows were 1.27±0.26 and 2.65±0.60 mL/g/min during rest and stress, while global MFR was 2.17 (Not shown).

Overall, no differences were observed for rest MBF (MBF_{rest}) (1.29 (± 0.29) vs 1.33 (± 0.29) mL/g/min,

Table 1. Baseline characteristics including cardiac risk markers

	Study population (*n* = 20)
Age, years (± SD)*	64 (± 9)
Family history of CVD, *n* (%)	6 (30%)
Current smoker, *n* (%)	2 (10%)
Previous smoker, *n* (%)	4 (20%)
Packyears, years (± SD)	31 (± 18)
SBP, mmHg (± SD)	159 (± 21)
DBP, mmHG (± SD)	89 (± 10)
BMI, kg/m^2 (± SD)	33 (± 15)
Hypercholesterolemia, *n* (%)	3 (15%)
Hypertension, *n* (%)	8 (40%)
Diabetes, *n* (%)	1 (5%)
ACE-inhibitors/Angiotensin II receptor blockers, *n* (%)	3 (15%)
Beta blockers, *n* (%)	1 (5%)
Calcium antagonist, *n* (%)	3 (15%)
Diuretics, *n* (%)	5 (25%)
Lipid lowering therapy, *n* (%)	3 (15%)
Years between RT and cardiac PET, years (± SD)	7 (± 2)

SD, Standard deviation; *CVD*, cardiovascular disease; *SBP*, systolic blood pressure; *DBP*, diastolic blood pressure; *BMI*, Body Mass Index; *RT*, radiotherapy; *PET*, positron-emission-tomography
*Age at cardiac PET examination

Table 2. Coronary Artery Calcium Scores

	CACS = 0	CACS = 1–400	CACS > 400
Study population (*n* = 18), *n* (%)	7 (39%)	9 (50%)	2 (11%)

CACS, Coronary Artery Calcium Score

Table 3. Blood flow and coronary flow reserves in the anterior vs inferior wall myocardium in ^{13}N-NH_3 myocardial perfusion PET

	Anterior wall	Inferior wall	*P*-value*
Blood flow (mL/g/min), rest (± SD)	1.29 (± 0.29)	1.33 (± 0.29)	NS
Blood flow (mL/g/min), stress (± SD)	2.74 (± 0.59)	2.78 (± 0.66)	NS
MFR (± SD)	2.22 (± 0.62)	2.17 (± 0.65)	NS

MFR, myocardial flow reserve; *NS*, non-significant
*Paired *t*-tests

P = ns), stress MBF (MBF_{stress}) (2.74 (± 0.59) vs 2.78 (± 0.66) mL/g/min, *P* = ns) or MFR (2.22 (± 0.62) vs 2.17 (± 0.65), *P* = ns) between anterior and inferior wall myocardium.

In one patient a mixed reversible and irreversible myocardial perfusion defect was detected in the anterior wall myocardium (Figure 5). This 69 year old patient with a BMI of 23 had a family history of CVD and hypertension since her thirties, but did not have hypercholesterolemia or diabetes and had never smoked.

DISCUSSION

The main findings of the present study were (1) In the 20 patients studied, no difference in MBF between the irradiated anterior and non-irradiated inferior wall myocardium could be detected at an average of 7 years after modern RT, but the sample size may have been too small to detect any differences and (2) only one of 20 patients presented a mixed reversible and irreversible myocardial perfusion defect. However, potentially the decrease in flow reserve may be seen later than our follow-up.

The quantitative MBF and MFR are reliable indices for evaluating functional severity, influenced by both epicardial stenosis and microvascular disease.[30] What was striking, was that the global MFR of the heart as a whole in our patients (mean global MFR 2.17) was well below the expected value in a normal population (MFR > 2.50).[31] Since CACS values were normal in our patients, epicardial stenosis to any serious extent seemed unlikely. Therefore, the globally reduced MFR may likely be indicative of a global microvascular dysfunction/disease. A significant proportion of our patients were exposed to adjuvant anthracycline prior to RT, whereas routine treatment with adjuvant trastuzumab was not yet established. Anthracycline is well known to have cardiotoxic side effects and therefore a plausible cause to the globally reduced MFR, although purely speculative, may well be due to cardiotoxic effects of chemotherapeutics. However, whether this is the case or if local irradiation of the anterior myocardium could have caused a global myocardial injury is unknown. Nevertheless and purely hypothesis generating, it would be reasonable to assume that a potential global injury would have been initiated from the part of the myocardium that received the highest radiation dose and thus to be measureable as a difference in MFR in the irradiated vs non-irradiated part of the myocardium. This was also what led to the design of the study, where each patient acted as their own control instead of utilizing a control group. In our patients, we did not find a difference between MFR in the irradiated anterior part of the myocardium and the non-irradiated inferior part and we could thus not detect an initiation spot for radiation-induced myocardial injury. However, radiation-induced myocardial injury may take decades to manifest and sub-detectable myocardial injury may still exist and slowly evolve into manifest myocardial injury in a decade or more. Nonetheless, our results still need confirmation in a larger study group with controls.

Much of our present knowledge comes from now outdated RT techniques, in which mean whole heart doses of 0.9-14 Gy for left-sided and 0.4-6 Gy for right-

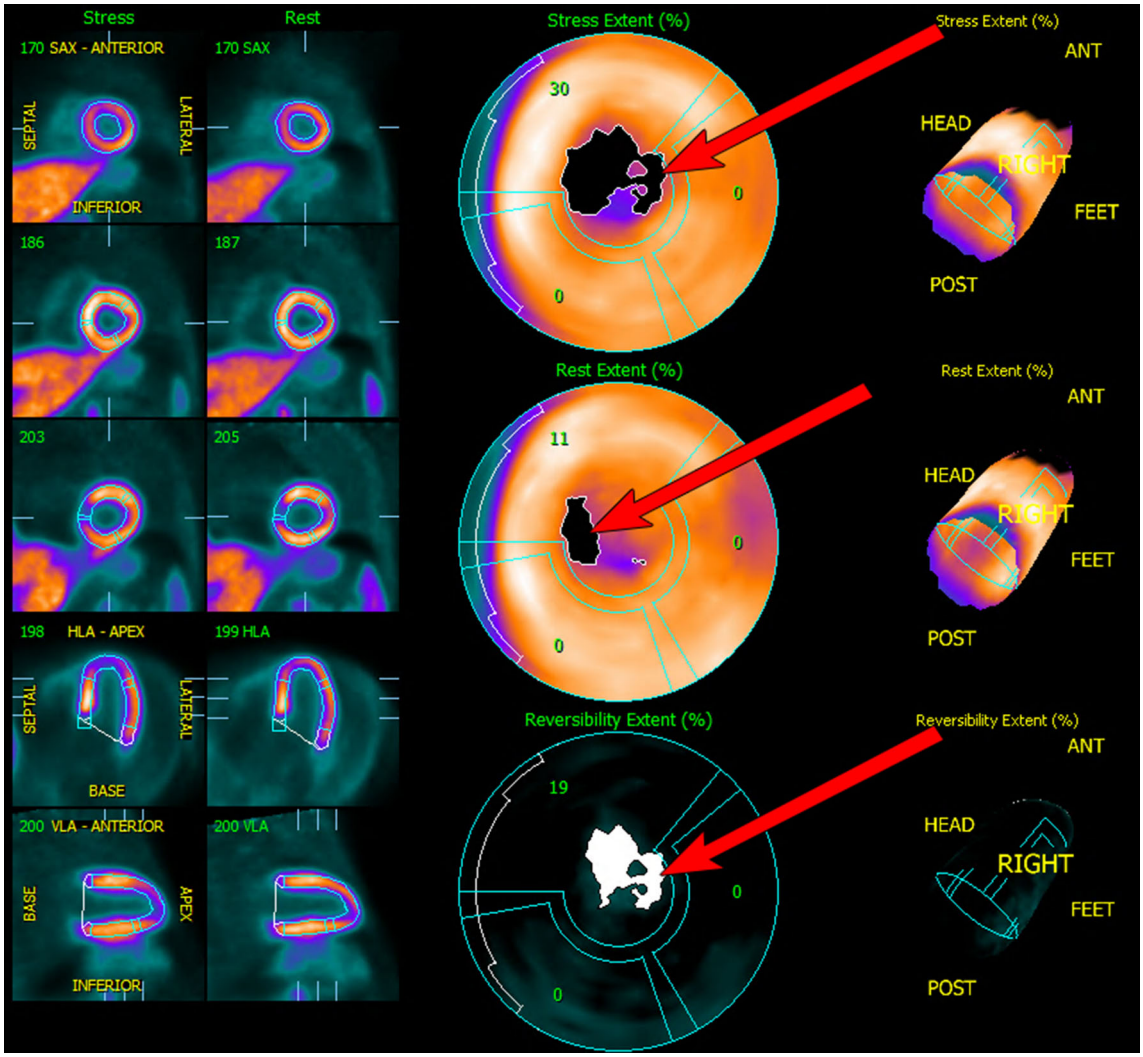

Figure 5. Rest and stress myocardial perfusion PET showing a mixed reversible and irreversible myocardial perfusion defect (red arrow) located to the irradiated anterior wall myocardium.

sided RT have been reported.[7,10] A clear dose-response relationship between mean heart radiation dose and cardiovascular risk exists, although there are large uncertainties for mean cardiac doses < 5 Gy.[32,33] However, the dose is distributed very unevenly in the heart, especially with the 3D-conformal irradiation techniques used in our cohort, and it is important to note that the mean heart dose is merely a surrogate measure for the size of the heart volume which is within the irradiated volume.[32,33] The highest radiation doses tend to be delivered to the anterior part of the heart, in particular the territory of the LAD artery.[10]

Clinical studies have shown a relationship between the extent of myocardial perfusion defects in non-symptomatic breast cancer survivors and volume of the left ventricle included in the radiation field.[34] Besides total radiation dose of $>$ 30-35 Gy, a higher dose per fraction ($>$ 2 Gy/day), presence of tumor next to the heart, younger age at exposure and time since exposure, type of radiation source (e.g. cobalt), cardiotoxic chemotherapy (e.g. anthracycline and trastuzumab) and other cardiac risk factors (e.g. diabetes, smoking etc.) have been reported as risk factors for radiation-induced cardiotoxicity.[35]

Since the introduction of modern 3-dimensional treatment planning and conformal RT techniques, the mean radiation doses to the heart have been reduced significantly. In a systematic review, reported average mean heart doses from tangential RT with breath control for left-sided breast cancer were down to 1.3 Gy (0.4-2.5 Gy).[7] However, some patients may still receive a higher dose, due to their specific anatomy (e.g. anterior heart,

or pectus excavatum). Several studies indicate that the lower dose associated with modern RT may lead to lower risks of radiation-induced heart disease. In a large register study, including 344,831 breast cancer patients treated with breast conserving surgery and modern adjuvant RT, the impact of tumor laterality on overall survival was examined to indirectly determine whether left-sided breast radiotherapy remains associated with increased cardiac mortality. After a median follow-up time of 6.04 years, overall survival was identical between left and right-sided breast cancers (Hazard Ratio (HR) = 1.002, $P = 0.874$). Even after restricting analyses to patients with at least 10 years of follow-up (27,725 patients), no difference by laterality in overall survival was found (breast RT only (HR = 0.955, $P = 0.368$), breast plus regional nodal RT (HR = 0.859, $P = 0.155$)). Researchers concluded that RT-induced cardiac disease may be less prominent than previously demonstrated.[36]

In a recent systematic review of six RT studies between 1996 and 2016, cardiac single-photon emission tomography (SPECT) was used to evaluate the rates of post-RT cardiac SPECT myocardial perfusion abnormalities and relate these to the irradiated left ventricular volume.[33] Reported perfusion defects were more often seen in the apical and anterolateral part of the left ventricle and could in three studies be correlated to the percentage of the left ventricle within the RT field. Contrary to these results, two studies using cardiac sparing techniques such as deep inspiration RT reported no perfusion defects in the myocardium. Thus there appears to be a strong dose/volume dependence between incidental radiation of the heart in left breast RT and detection of early post-RT perfusion defects, supporting the use of techniques to reduce cardiac exposure.[33]

Coronary artery calcification score is another surrogate marker and early indicator of coronary atherosclerosis. In our study, patients had a median coronary artery calcium score of 4, considered normal for a population with a mean age of 64 ± 9 years.[37] Calcifications were primarily located in the LAD and thus located in the field of radiation. This, on the other hand, is not unusual since LAD is the most common location for coronary artery calcifications (CAC). Unfortunately, CACS were not measured before RT which would have made it possible to follow the progression of CACS in the irradiated LAD and the non-irradiated RCA. In conclusion, to what extent calcification was driven simply by age and to what extent it was driven by irradiation remains unknown. This is, however, something that has been investigated in other studies and the results of these studies corroborate our myocardial blood flow findings. In a study, 333 breast cancer survivors were divided into two groups according to RT ($n = 54$) or no-RT ($n = 279$). Mean age at diagnosis was similar in the RT- and no-RT-group (57.4 ± 13.1 vs 58.0 ± 11.9 years, $P = 0.771$) and no difference in race, smoking history, cancer laterality or cancer stage was found. After a median time of 2 years after RT/no-RT, no difference in median CAC burden between the two groups ($P = 0.982$) was detected. Researchers concluded that breast cancer survivors receiving RT were not more likely to show CAC on follow-up CT imaging.[38]

In another CAC study, a prospective longitudinal study, CACS were measured prior to and 3 years after RT in 99 breast cancer patients. Three groups were compared: patients receiving left-sided RT, right-sided RT and left-sided RT with breath-hold. CACS were analyzed as overall CACS, but also as a LAD CACS in the irradiated anterior part of the heart and a RCA CACS in the non-irradiated part. Although limited by small sample size and relatively short follow-up period, patients receiving breath-hold-based RT showed a less pronounced increase in overall CACS three years after RT. Furthermore, LAD CACS increased more in patients receiving left-sided RT without breath-hold compared to patients receiving right-sided RT and left-sided RT with breath-hold. In conclusion, breathing adapted RT for breast cancer seems to lead to a less pronounced increase in CAC.[39]

NEW KNOWLEDGE GAINED

Most of our current knowledge about RT-induced heart disease is based on data from outdated radiation therapy techniques. Hence, there is a need for data based on more contemporary RT techniques. This is, to our knowledge, the first study to directly measure and compare blood flows via ^{13}N-NH_3 PET in irradiated vs non-irradiated myocardium in breast cancer patients following modern RT. Global myocardial flow reserves were significantly lower than expected, in our study, presumably due to adjuvant anthracycline treatment, but we did not find a difference between the irradiated vs non-irradiated myocardium. Therefore, our results indicate, and thus corroborate more recent studies, that myocardial injury associated with modern RT may be considerably lower than with older RT techniques. There is however still a need for a larger study to confirm our results.

LIMITATIONS

Since patients did not undergo myocardial perfusion PET imaging and coronary artery calcium score scan before RT, our study was limited to show cross-sectional outcomes rather than longitudinal changes in CAC and

MBF. The lack of clinical follow-up is also a limitation. Furthermore, we acknowledge the fact that this was a small study and that the period between RT treatment and myocardial perfusion PET might be too short to show potential myocardial injury.

CONCLUSION

Even though our sample size may be too small to warrant an unambiguous conclusion, at least early signs of cardiac injury detected by NH_3 myocardial perfusion PET was not frequent in our cohort of patients treated with a modern radiation therapy technique for left-sided breast cancer, even seven years after treatment. These findings however, may still not rule out development of myocardial injury in a decade or later.

Disclosures

ANP has nothing to disclose. LS has the following disclosures: Member of advisory board and principal investigator, Takeda; Member of advisory board, Merck; Research agreement, Varian Medical Systems and Merck Serono; Principal investigator, Nanovi. MCA has the following disclosures Research agreement, Varian Medical Systems. PH has nothing to disclose. All other authors declare no conflict of interest.

References

1. Ferlay J, Soerjomataram I, Ervik M, et al. GLOBOCAN 2012 v1.1, Cancer Incidence and mortality worldwide: IARC CancerBase No. 11. Lyon, France: International Agency for Research on Cancer; 2014. http://globocan.iarc.fr/Pages/fact_sheets_population.aspx. Accessed 3 Aug 2018
2. Clarke M, Collins R, Darby S, et al. Effects of radiotherapy and of differences in the extent of surgery for early breast cancer on local recurrence and 15-year survival: An overview of the randomised trials. Lancet 2005;366:2087-106.
3. Poortmans PM, Collette S, Kirkove C, et al. Internal mammary and medial supraclavicular irradiation in breast cancer. N Engl J Med 2015;373:317-27.
4. Whelan TJ, Olivotto IA, Levine MN. Regional nodal irradiation in early-stage breast cancer. N Engl J Med 2015;373:1878-9.
5. Thorsen LB, Offersen BV, Dano H, et al. DBCG-IMN: A population-based cohort study on the effect of internal mammary node irradiation in early node-positive breast cancer. J Clin Oncol 2016;34:314-20.
6. Aznar MC, Duane FK, Darby SC, et al. Exposure of the lungs in breast cancer radiotherapy: A systematic review of lung doses published 2010–2015. Radiother Oncol 2018;126:148-54.
7. Taylor CW, Wang Z, Macaulay E, et al. Exposure of the heart in breast cancer radiation therapy: A systematic review of heart doses published during 2003 to 2013. Int J Radiat Oncol Biol Phys 2015;93:845-53.
8. McGowan JV, Chung R, Maulik A, et al. Anthracycline chemotherapy and cardiotoxicity. Cardiovasc Drugs Ther 2017;31:63-75.
9. Early Breast Cancer Trialists' Collaborative Group, Darby S, McGale P, et al. Effect of radiotherapy after breast-conserving surgery on 10-year recurrence and 15-year breast cancer death: Meta-analysis of individual patient data for 10,801 women in 17 randomised trials. Lancet 2011;378:1707-16.
10. Taylor CW, Nisbet A, McGale P, et al. Cardiac exposures in breast cancer radiotherapy: 1950s–1990s. Int J Radiat Oncol Biol Phys 2007;69:1484-95.
11. Darby SC, McGale P, Taylor CW, et al. Long-term mortality from heart disease and lung cancer after radiotherapy for early breast cancer: Prospective cohort study of about 300,000 women in US SEER cancer registries. Lancet Oncol 2005;6:557-65.
12. Harris EE. Cardiac mortality and morbidity after breast cancer treatment. Cancer Control 2008;15:120-9.
13. Moreira LA, Silva EN, Ribeiro ML, et al. Cardiovascular effects of radiotherapy on the patient with cancer. Rev Assoc Med Bras 2016;62:192-6.
14. Marks LB, Yu X, Prosnitz RG, et al. The incidence and functional consequences of RT-associated cardiac perfusion defects. Int J Radiat Oncol Biol Phys 2005;63:214-23.
15. Pierce LJ, Butler JB, Martel MK, et al. Postmastectomy radiotherapy of the chest wall: Dosimetric comparison of common techniques. Int J Radiat Oncol Biol Phys 2002;52:1220-30.
16. Taylor CW, Povall JM, McGale P, et al. Cardiac dose from tangential breast cancer radiotherapy in the year 2006. Int J Radiat Oncol Biol Phys 2008;72:501-7.
17. Lu HM, Cash E, Chen MH, et al. Reduction of cardiac volume in left-breast treatment fields by respiratory maneuvers: A CT study. Int J Radiat Oncol Biol Phys 2000;47:895-904.
18. Sixel KE, Aznar MC, Ung YC. Deep inspiration breath hold to reduce irradiated heart volume in breast cancer patients. Int J Radiat Oncol Biol Phys 2001;49:199-204.
19. Remouchamps VM, Vicini FA, Sharpe MB, et al. Significant reductions in heart and lung doses using deep inspiration breath hold with active breathing control and intensity-modulated radiation therapy for patients treated with locoregional breast irradiation. Int J Radiat Oncol Biol Phys 2003;55:392-406.
20. Pedersen AN, Korreman S, Nystrom H, et al. Breathing adapted radiotherapy of breast cancer: Reduction of cardiac and pulmonary doses using voluntary inspiration breath-hold. Radiother Oncol 2004;72:53-60.
21. Korreman SS, Pedersen AN, Aarup LR, et al. Reduction of cardiac and pulmonary complication probabilities after breathing adapted radiotherapy for breast cancer. Int J Radiat Oncol Biol Phys 2006;65:1375-80.
22. Goethals I, Dierckx R, De Meerleer G, et al. The role of nuclear medicine in the prediction and detection of radiation-associated normal pulmonary and cardiac damage. J Nucl Med 2003;44:1531-9.
23. Prosnitz RG, Hubbs JL, Evans ES, et al. Prospective assessment of radiotherapy-associated cardiac toxicity in breast cancer patients: Analysis of data 3 to 6 years after treatment. Cancer 2007;110:1840-50.
24. Juneau D, Erthal F, Ohira H, et al. Clinical PET myocardial perfusion imaging and flow quantification. Cardiol Clin 2016;34:69-85.
25. Taylor C, Correa C, Duane FK, et al. Estimating the Risks of breast cancer radiotherapy: Evidence from modern radiation doses to the lungs and heart and from previous randomized trials. J Clin Oncol 2017;35:1641-9.
26. Greenland P, Bonow RO, Brundage BH, et al. ACCF/AHA 2007 clinical expert consensus document on coronary artery calcium scoring by computed tomography in global cardiovascular risk assessment and in evaluation of patients with chest pain: A report

of the American College of Cardiology Foundation Clinical Expert Consensus Task Force (ACCF/AHA Writing Committee to Update the 2000 Expert Consensus Document on Electron Beam Computed Tomography) developed in collaboration with the Society of Atherosclerosis Imaging and Prevention and the Society of Cardiovascular Computed Tomography. J Am Coll Cardiol 2007;49:378-402.
27. Hutchins GD, Schwaiger M, Rosenspire KC, et al. Noninvasive quantification of regional blood flow in the human heart using N-13 ammonia and dynamic positron emission tomographic imaging. J Am Coll Cardiol 1990;15:1032-42.
28. American Society of Nuclear Cardiology. Imaging guidelines for nuclear cardiology procedures, part 2. J Nucl Cardiol 1999;6:G47-84.
29. Damkjaer SM, Aznar MC, Pedersen AN, et al. Reduced lung dose and improved inspiration level reproducibility in visually guided DIBH compared to audio coached EIG radiotherapy for breast cancer patients. Acta Oncol 2013;52:1458-63.
30. Kiso KSE, Watabe H, Kanai Y, Fujino K, Hatazawa J. Normal values of myocardial blood flow and myocardial flow reserve evaluated by 3-dimensional dynamic PET/CT system with ^{13}N-ammonia. J Radiol Radiat Ther 2013;1:1016.
31. Schindler TH, Schelbert HR, Quercioli A, et al. Cardiac PET imaging for the detection and monitoring of coronary artery disease and microvascular health. JACC Cardiovasc Imaging 2010;3:623-40.
32. Stewart FA. Mechanisms and dose-response relationships for radiation-induced cardiovascular disease. Ann ICRP 2012;41:72-9.
33. Kaidar-Person O, Zagar TM, Oldan JD, et al. Early cardiac perfusion defects after left-sided radiation therapy for breast cancer: is there a volume response? Breast Cancer Res Treat 2017;164:253-62.
34. Stewart FA, Hoving S, Russell NS. Vascular damage as an underlying mechanism of cardiac and cerebral toxicity in irradiated cancer patients. Radiat Res 2010;174:865-9.
35. Jaworski C, Mariani JA, Wheeler G, et al. Cardiac complications of thoracic irradiation. J Am Coll Cardiol 2013;61:2319-28.
36. Rutter CE, Chagpar AB, Evans SB. Breast cancer laterality does not influence survival in a large modern cohort: Implications for radiation-related cardiac mortality. Int J Radiat Oncol Biol Phys 2014;90:329-34.
37. Hoff JA, Chomka EV, Krainik AJ, et al. Age and gender distributions of coronary artery calcium detected by electron beam tomography in 35,246 adults. Am J Cardiol 2001;87:1335-9.
38. Takx RAP, Vliegenthart R, Schoepf UJ, et al. Coronary artery calcium in breast cancer survivors after radiation therapy. Int J Cardiovasc Imaging 2017;33:1425-31.
39. Mast ME, Heijenbrok MW, van Kempen-Harteveld ML, et al. Less increase of CT-based calcium scores of the coronary arteries: Effect three years after breast-conserving radiotherapy using breath-hold. Strahlenther Onkol 2016;192:696-704.

Publisher's Note Springer Nature remains neutral with regard to jurisdictional claims in published maps and institutional affiliations.